Elsevier Editorial System(tm) for Plant Physiology and Biochemistry

Manuscript Draft

Manuscript Number: PLAPHY-D-17-00240R1

Title: Structural changes in cell wall pectins during strawberry fruit development

Article Type: Research Paper

Keywords: Atomic force microscopy; cell wall; Fragaria × ananassa; fruit ripening; fruit softening; pectins.

Corresponding Author: Dr. Jose A. Mercado,

Corresponding Author's Institution: Universidad de Malaga

First Author: Candelas Paniagua

Order of Authors: Candelas Paniagua; Nieves Santiago-Domenech; Andrew R. Kirby; A. Patrick Gunning; Victor J. Morris; Miguel A. Quesada; Antonio J. Matas; Jose A. Mercado

Abstract: Strawberry (Fragaria × anannasa Duch.) is one of the most important soft fruit. Rapid loss of firmness occurs during the ripening process, resulting in a short shelf life and high economic losses. To get insight into the role of pectin matrix in the softening process, cell walls from strawberry fruit at two developmental stages, unripe-green and ripe-red, were extracted and sequentially fractionated with different solvents to obtain fractions enriched in a specific component. The yield of cell wall material as well as the per fresh weight contents of the different fractions decreased in ripe fruit. The largest reduction was observed in the pectic fractions extracted with a chelating agent (trans-1,2- diaminocyclohexane-N,N,N'N'-tetraacetic acid, CDTA fraction) and those covalently bound to the wall (extracted with Na2CO3). Uronic acid content of these two fractions also decreased significantly during ripening, but the amount of soluble pectins extracted with phenol:acetic acid:water (PAW) and water increased in ripe fruit. Fourier transform infrared spectroscopy of the different fractions showed that the degree of esterification decreased in CDTA pectins but increased in soluble fractions at ripen stage. The chromatographic analysis of pectin fractions by gel filtration revealed that CDTA, water and, mainly PAW polyuronides were depolymerised in ripe fruit. By contrast, the size of Na2CO3 pectins was not modified. The nanostructural characteristics of CDTA and Na2CO3 pectins were analysed by atomic force microscopy (AFM). Isolated pectic chains present in the CDTA fractions were significantly longer and more branched in samples from green fruit than those from red fruit. No differences in contour length were observed in Na2CO3 strands between samples of both stages. However, the percentage of branched chains decreased from 19.7 % in unripe samples to 3.4 % in ripe fruit. The number of pectin aggregates was higher in green fruit samples of both fractions. These results show that the nanostructural complexity of pectins present in CDTA and Na2CO3 fractions diminishes during fruit development, and this correlates with the solubilisation of pectins and the softening of the fruit.

Cover Letter

May, 11 2017

Dear Editor

Please find enclosed the revised version of our ms number PLAPHY-D-17-00240 entitled "Structural changes in cell wall pectins during strawberry fruit development" by Paniagua et al.

Changes made in the manuscript are labelled in red.

Looking forward to hearing from you

José A. Mercado

Dep. Biología Vegetal

Universidad de Málaga

Structural changes in cell wall pectins during strawberry fruit development

Candelas Paniagua[a], Nieves Santiago-Doménech[a], Andrew R. Kirby[b], A. Patrick Gunning[b], Victor J. Morris[b], Miguel A. Quesada[c], Antonio J. Matas[a], José A. Mercado[a]

[a]Instituto de Hortofruticultura Subtropical y Mediterránea "La Mayora" (IHSM-UMA-CSIC), Departamento de Biología Vegetal, Universidad de Málaga, 29071, Málaga, Spain.

[b] Institute of Food Research, Norwich Research Park, Colney, Norwich, NR4 7UA, UK.

[c]Departamento de Biología Vegetal, Universidad de Málaga, 29071, Málaga, Spain.

Corresponding author:

José A. Mercado

Instituto de Hortofruticultura Subtropical y Mediterránea "La Mayora" (IHSM-UMA-CSIC), Departamento de Biología Vegetal, Universidad de Málaga, 29071, Málaga, Spain.

e-mail: mercado@uma.es

Abstract

Strawberry (*Fragaria* × *anannasa* Duch.) is one of the most important soft fruit. Rapid loss of firmness occurs during the ripening process, resulting in a short shelf life and high economic losses. To get insight into the role of pectin matrix in the softening process, cell walls from strawberry fruit at two developmental stages, unripe-green and ripe-red, were extracted and sequentially fractionated with different solvents to obtain fractions enriched in a specific component. The yield of cell wall material as well as the per fresh weight contents of the different fractions decreased in ripe fruit. The largest reduction was observed in the pectic fractions extracted with a chelating agent (trans-1,2- diaminocyclohexane-N,N,N'N'-tetraacetic acid, CDTA fraction) and those covalently bound to the wall (extracted with Na_2CO_3). Uronic acid content of these two fractions also decreased significantly during ripening, but the amount of soluble pectins extracted with phenol:acetic acid:water (PAW) and water increased in ripe fruit. Fourier transform infrared spectroscopy of the different fractions showed that the degree of esterification decreased in CDTA pectins but increased in soluble fractions at ripen stage. The chromatographic analysis of pectin fractions by gel filtration revealed that CDTA, water and, mainly PAW polyuronides were depolymerised in ripe fruit. By contrast, the size of Na_2CO_3 pectins was not modified. The nanostructural characteristics of CDTA and Na_2CO_3 pectins were analysed by atomic force microscopy (AFM). Isolated pectic chains present in the CDTA fractions were significantly longer and more branched in samples from green fruit than those from red fruit. No differences in contour length were observed in Na_2CO_3 strands between samples of both stages. However, the percentage of branched chains decreased from 19.7 % in unripe samples to 3.4 % in ripe fruit. The number of pectin aggregates was higher in green fruit samples of both fractions. These results show that the nanostructural complexity of pectins

present in CDTA and Na_2CO_3 fractions diminishes during fruit development, and this correlates with the solubilisation of pectins and the softening of the fruit.

Keywords: Atomic force microscopy, cell wall, *Fragaria* × *ananassa*, fruit ripening, fruit softening, pectins

1. Introduction

Ripening of fleshy fruit is a combination of physiological and biochemical processes that make edible fruit more attractive to seed dispersal organisms (Gapper et al., 2013). In soft fruit such as strawberry, the rapid loss of firm texture is one of the most noticeable changes during ripening, but it poses a major problem to strawberry growers due to the short postharvest life of this commodity. It is generally accepted that the modification of the physical and chemical features of parenchyma cell walls and the loss of intercellular adhesion resulting from the dissolution of the middle lamella are the major determining factors of fruit softening (Brummell, 2006; Goulao and Oliveira, 2008; Mercado et al., 2011). Nevertheless, the biochemical mechanisms underlying softening are not completely clear.

Strawberry softening is characterised by an increase in pectin solubilisation, i.e. an increase in the amount of pectins loosely bound to the cell wall, extracted with water but also with chelating agents such as CDTA in some cultivars (Huber, 1984; Koh and Melton, 2002; Posé et al., 2011). The increasing levels of soluble pectins is paralleled with a decrease in the amount of covalently bound pectins, those supposedly located in the primary cell wall, mainly extracted with sodium carbonate (Posé et al., 2011). Several hypotheses about the causes of pectin solubilisation during fruit ripening have been proposed (Paniagua et al., 2014). One of them relies on the loss of arabinan and galactan side chains from rhamnogalacturonan I (RGI) (Gross and Sams, 1984;

Redgwell et al., 1997a), weakening the cell wall network. Moreover, the loss of neutral sugars might also increase the cell wall porosity, which could facilitate the access of pectinases to their substrates (Smith et al., 2002). In accordance with this, the silencing of a β-galactosidase gene reduced strawberry fruit softening and this was related to a lower pectin solubilisation and an increased content of galactose in cell walls (Paniagua et al., 2016). However, not all the types of fruit show a correlation between the loss of neutral sugar residues and pectin solubilisation (Redgwell et al., 1997a).

As an alternative hypothesis, depolymerisation of chelated and/or covalently bound pectins as result of the action of pectinases, e.g. polygalacturonase, pectin methyl esterase or pectate lyase, may facilitate the solubilisation of pectic components not previously present in the soluble fractions (Redgwell et al., 1997b; Rose et al., 1998; Vicente et al., 2005). In strawberry, the role of pectin depolymerisation in fruit softening is unclear. Some authors did not find changes in the average molecular weight of polyuronides during strawberry ripening (Huber, 1984; Redgwell et al., 1997a; Lee et al., 2011) while others observed a significant depolymerisation of bound pectins, depending on the cultivar studied (Rosli et al., 2004). Although there is not a general consensus about the importance of polyuronide depolymerisation, functional analyses of genes encoding pectin degrading enzymes suggest a key role of this process in the changes in texture taking place during strawberry development. Thus, the down-regulation of a pectate lyase or a polygalacturonase gene by antisense transformation increased strawberry fruit firmness at the red stage and improved postharvest shelf life (Jiménez-Bermúdez et al., 2002; Quesada et al., 2009).

Most studies dealing with the role of pectins in strawberry fruit texture analysed polyuronides by classical techniques such as size exclusion chromatography. Recently, Posé et al. (2015) used atomic force microscopy (AFM) to characterize the effect of

pectate lyase and polygalaturonase genes silencing in pectin nanostructure. They found that down-regulation of both genes increased pectin chains length and their structural complexity, the magnitude of these changes being correlated with the increase in fruit firmness.

The main objective of this research was to analyse and compare the cell wall complexity in green and red strawberry fruit, focusing the structural changes that occurs in the chelated and covalently bound pectin fractions.

2. Materials and methods

2.1. Plant material

Strawberry (*Fragaria* × *ananassa* Duch., cv. 'Chandler') plants obtained by runner propagation were grown in 22 cm diameter pots containing a mixture of peat moss, sand and perlite (6:3:1). These plants were cultured in a greenhouse until fruiting, under natural photoperiod and temperature conditions. Fruit were collected from March to June. After harvest, fruit were immediately frozen in liquid nitrogen and stored at -25 ºC until used. Two developmental stages were selected, green-unripe and red-ripe (Fig.1A). Fruit from the green stage were about 1 cm in diameter displaying both green receptacle and green achenes. Ripe red fruit were characterized by its fully red receptacle and soft texture.

2.2. Cell wall extraction and fractionation

Achenes from frozen fruit were removed and the cell wall from fruit receptacles was extracted following the method of Redgwell et al. (1992), as modified by Santiago-Doménech et al. (2008). This procedure yielded cell wall material (CWM) and polymers soluble in PAW (phenol:acetic acid:water, 2:1:1, w:v:v), solvent used to inactivate

enzymes (PAW fraction). The CWM (80 mg) was sequentially extracted following the procedure of Santiago-Doménech et al. (2008) to obtain fractions enriched in pectins (water, CDTA and sodium carbonate solubilised fractions) and two hemicellulose enriched fractions extracted with 1M KOH and 4M KOH. Pectin fractions to be analysed by AFM were stored until required at -20 ºC as aqueous solutions, in order to avoid possible aggregation induced by freeze-drying.

The uronic acid (UA) content in PAW and cell wall fractions was measured by the carbazol method as reported by Filisetti-Cozzi and Carpita (1991), using GalA as standard. The total neutral sugar content was determined by the orcinol method (Rimington, 1931) using glucose as standard. For neutral sugars analysis of CDTA and Na_2CO_3 fractions, samples were hydrolysed with 72 % (w/w) sulphuric acid. After neutralization with ammonia, carbohydrates were derivatised to alditol acetates and analysed by gas chromatography with flame ionization detection (Blakeney et al., 1983). GC analysis was carried out in triplicate.

2.3. Fourier transform infrared spectroscopy

Dried samples were used to capture the infrared spectra with an Attenuated Total Reflectance (ATR) accessory (MIRacle ATR, PIKE Technologies, USA) coupled to a Fourier transform infrared (FTIR) spectrometer (FT/IR-4100, JASCO, Spain). The samples were processed as described by Posé et al. (2012) and the spectra were collected in the 4000–600 cm^{-1} range with a resolution of 4 cm^{-1} and averaged over 25 scans per sample.

2.4. Size exclusion chromatography

The gel filtration chromatography measurements were performed as described previously by Santiago-Doménech et al. (2008). Briefly, pectin fractions were loaded onto a 40 cm height × 10 mm internal diameter column filled with Sepharose (Sigma-Aldrich Química SA, Spain) CL6B for PAW and water fractions or CL2B for CDTA and sodium carbonate pectins. Gel medium was equilibrated with 0.2 M acetate buffer, pH 5, for PAW, water and CDTA fractions, or 0.1 M TRIS-HCl buffer, pH 8.4, for sodium carbonate samples. Samples, 6-8 mg, were dissolved in the corresponding equilibration buffer, loaded on the column and eluted at a 14 mL h^{-1} flow rate. Blue dextran standard (2000 kDa) and acetone were used for column calibration. Fractions (1 mL) were collected and assayed for uronic acids (Filisetti-Cozzi and Carpita,1991).

2.5. Atomic force microscopy

The ionically and covalently-bound pectin fractions, corresponding to CDTA and sodium carbonate soluble polymers, respectively, were analysed by AFM as described by Posé et al. (2012). Briefly, samples were diluted in water to a concentration of 2-4 mg L^{-1}. Then, 3 μL were pipetted onto freshly-cleaved mica and dried over a heating block at 37 ºC. The sample was then inserted into the liquid cell of the AFM microscope (manufactured by ECS, East Coast Scientific, Cambridge, UK) and visualized under re-distilled butanol. Butanol was used as an imaging solvent to limit desorption of the molecules from the substrate and to eliminate capillary condensation effects (Kirby et al., 1996; Round et al., 2001). Short tip variety AFM probe model contact cantilevers (Budget Sensors, Bulgaria) were used with a 13 kHz resonance frequency and a 0.4 N m^{-1} force constant. The samples were scanned in contact mode at a frequency of 2 Hz. More than 30 images with an area 1 μm^2 were collected for each sample.

2.6. AFM image analysis

The ECS software (SPM 6.01, Cambridge, UK) was used for chain height analysis (Kirby et al., 1996). The height of the chains was used to differentiate true branch points from entangled chains. Further analyses were applied offline. Initially, the original AFM files were converted to TIFF files using Paint Shop Pro v. 5.00 software. Image contrast and stripe correction were optimized using Gwyddion v2.32 software. Contour length measurements, defined as total length including backbone and branches, were analysed by plotting the length of the chains with the freehand tool of ImageJ software (Adams et al., 2003; Posé et al., 2012). Individual molecules were defined as strands that were not entangled with, or overlapping other strands, that were long enough to be exactly visualized, and which lay entirely within the scanned area (Adams et al., 2003). A minimum of 600 chains were measured per sample and the results represented as frequency histograms. Number-average (L_N) and weight-average (L_W) contour lengths, as well as polydispersity index (PDI) calculated as the ratio L_W/L_N, were estimated as described previously (Posé et al., 2012).

2.7. Statistical analysis

The SPSS software (v.23) was used for statistical analyses. Data were analysed by ANOVA and mean separation was done by Tukey-HSD. The Levene test for homogeneity of variances was performed prior to ANOVA. For AFM statistical analyses, thirty images per sample were collected to obtain representative data of the pectin samples. The median from the original data distributions were compared with the non-parametric Kruskal–Wallis test. Differences in the branching of the polymer chains, presence/absence of side chains, were analysed by Chi-square test. All statistical tests were performed at $P = 0.05$.

3. Results

3.1 Cell wall yield and fractionation

The yield of CWM per weight of tissue on a fresh weight basis was around three times higher in unripe than ripe fruit, 34 vs 9 g kg^{-1}, respectively. No significant differences were found in the amount of polymers solubilised with PAW between green and red fruit extracts, yielding a mean PAW value of 0.6 g kg^{-1} of fruit. However, the ratio PAW:CWM increased from 0.017 in the green stage to 0.67 in ripe fruit. CWM was sequentially extracted with different solvents to obtain cell wall fractions enriched in specific polymers. The amount of the fractions rich in pectins, i.e. CDTA and Na_2CO_3, decreased significantly in ripe fruit (Fig. 1B). By contrast, the weight of fractions rich in hemicellulosic material, solubilised by KOH 1 M and 4 M, as well as the water fraction decreased slightly in red fruit, but these differences were not statistically significant (Fig. 1B).

The uronic acid (UA) content in the different cell wall fractions is shown in Fig. 2A. In both fruit stages, the highest amount of UA was observed in the CDTA fraction followed by the sodium carbonate fraction. As expected, the lowest pectic contents were obtained in both KOH fractions. Uronic acid content in the water soluble fraction was significantly higher in red fruit than in green fruit. Conversely, ripe fruit showed reduced amounts of UA in all the other fractions, especially in CDTA and sodium carbonate fractions (Fig. 2A). As regards PAW fraction, the amount of UA increased with ripening from 0.17±0.03 g kg^{-1} of fruit to 0.53±0.05 g kg^{-1}. The contents of neutral sugars decreased notably in CDTA, sodium carbonate and 4M KOH fractions in red fruit but remained at similar levels in both stages in the cases of water and 1M KOH fractions (Fig. 2B).

3.2 ATR-FTIR analysis

The cell wall fractions enriched in pectins from unripe and ripe fruit were analysed by ATR-FTIR and the spectra obtained are shown in Fig. 3. Main differences between both developmental stages for some fractions were observed in the region 1200-950 cm^{-1}, the typical fingerprint of polysaccharides, and in the ratio 1735/1600 cm^{-1}, indicative of the degree of pectin methylesterification. In the PAW fraction from green fruit, the peak at 1735 cm^{-1} arising from the ester carbonyl stretching band was low and by contrast the absorption band at around 1600 cm^{-1} was higher due to the asymmetric and symmetric COO^- stretching bands. The peak at 1735 cm^{-1} increased in ripe fruit suggesting a higher degree of esterification in the PAW fraction as the fruit ripen. A similar result was obtained in the water fraction. However, the spectral profiles of CDTA fractions suggest that the degree of methylation decreased from green to red fruit. As expected, the peak at 1735 cm^{-1} in the carbonate fraction disappeared as a result of the elimination of ester linkages during the alkaline extraction.

In the fingerprint region, 1200-950 cm^{-1}, of both water and CDTA spectral profiles from green and red fruit, main peaks were observed at 1097 and 1015 cm^{-1}, absorption bands typical of polygalacturonic acid. Carbonate profiles also showed the strongest peak at 1015 cm^{-1}; however, the band at 1097 cm^{-1} diminished whereas bands at 1075, 1050 and 953 cm^{-1} increased. This result suggests a different carbohydrate composition of the carbonate fraction which is probably enriched in neutral sugars (Kacuráková et al., 2000). Interestingly, the higher intensity of 1015 cm^{-1} band in the carbonate spectrum from red fruit when compared with green fruit suggests a decrease in the amount of neutral sugars in the carbonate fraction as the fruit ripen. It is noticeable that the fingerprint region of PAW fraction from red fruit was similar to the one observed in

carbonate fraction at the ripe stage. However, the PAW FTIR spectrum from green fruit showed a broad peak with a maximum at 1038 cm^{-1}, but low absorption at 1097, 1015 and 1143 cm^{-1}, indicating a minor amount of polygalacturonic acid in this fraction at this stage.

3.3 Size exclusion chromatography of pectin fractions

Chromatographic profiles of pectic polymers present in the pectin enriched fractions in unripe and ripe fruit are shown in Fig. 4. In unripe fruit, PAW and water-soluble polyuronides showed a main peak at the beginning of the profile that eluted at 13 mL, close to the elution volume of blue dextran but with a lower molecular mass than 2000 kDa. This main peak was followed by a tail of lower molecular mass pectins extending throughout the separation range of the column. This tail was more complex in the case of the profile of the water fraction obtained from green fruit which contained a higher representation of small molecular mass pectins. A clear decrease on the average molecular mass of PAW soluble polymers was observed in ripe fruit as reflected by the displacement of the main pectic peak to higher elution volumes, and the enrichment of the profile with middle size pectins, eluting between 15 and 25 mL. Similarly, the main peak eluting at 13 mL in water fraction from unripe fruit was displaced to the right in ripe fruit and the lower molecular mass peaks disappeared, suggesting a depolymerisation of these polyuronides during fruit development.

Polymers present in the CDTA fraction eluted throughout the fractionation range of the column. In unripe fruit, three main peaks at 17, 19 and 22.5 mL elution volumes were observed (Fig. 4). These main peaks were displaced towards lower molecular mass in ripe fruit. As regards sodium carbonate soluble pectins, a similar displacement was observed in the first peak, which eluted at 11.5 mL vs 12.5 mL in samples from green

and red fruit, respectively. A second broader peak of polymers, eluting between 20 and 27 mL, was observed at both developmental stages with minor differences between both type of fruit.

3.4. Neutral sugar composition of CDTA and sodium carbonate pectin fractions

Composition of neutral sugars in CDTA and sodium carbonate fractions in unripe and ripe fruit is shown in Fig. 5. Arabinose and galactose were the most abundant carbohydrates in both pectin fractions, accounting for more than 85 % of neutral sugars. The proportion of Ara decreased notably as the fruit ripen, especially in the sodium carbonate fraction. By contrast, the percentage of Gal was not modified in CDTA fraction and increased in the carbonate fraction during ripening. Considering both carbohydrates, the mol % of Ara plus Gal decreased by 21 % and 14 % in CDTA and sodium carbonate fractions, respectively.

3.5. AFM analysis of CDTA and sodium carbonate pectin fractions

CDTA and sodium carbonate soluble polymers were analysed at the nanostructural level by AFM since these two fractions contained the highest amount of pectins. Representative topographical AFM images of CDTA pectins from unripe and ripe fruit are shown in Fig.6. Zoomed images of the different structures visualized in AFM samples are shown in Fig.6A-F. Linear filamentous chains with few side chains were mainly present in CDTA samples at both developmental stages. Apparently, the isolated pectic chains were longer in unripe fruit samples. In addition, polymer aggregates with micellar-like appearance were more frequent in unripe fruit samples. Contrary to CDTA pectins, topographical AFM images from sodium carbonate soluble polymers did not show significant differences in the contour length of isolated pectic chains from unripe

and ripe fruit samples. However, branched chains and aggregate structures were more frequently observed in unripe samples.

Contour lengths of isolated polymer chains at both developmental stages were recorded. The length distributions in CDTA fraction were in the range 25 to 533 nm and 18 to 277 nm, in unripe and ripe fruit samples, respectively (Fig. 7). Conversely, the length distribution of Na_2CO_3 pectin samples ranged between 9 and 305 nm in unripe samples and 10 to 255 nm in ripe fruit (Fig. 7). In both fractions, the range of length distribution was wider for green fruit samples, including pectic isolated chains longer than 300 nm in CDTA fraction and 275 nm in sodium carbonate fraction. These longer chains were not present in the samples of the ripe stage. Furthermore, CDTA samples from unripe fruit showed a higher proportion of middle-sizes chains within the classes ranged from 75 to 150 nm; however, in samples from red fruit the frequencies of chains within this range decreased and an evident increase of the frequencies of chain in classes 50 and 75 nm was observed.

The number-average (L_N), weight-average (L_W) and polydispersity indexes (PDI) for the shape of contour length distributions are shown in Table 1. The median, as a more appropriate average for asymmetrical distributions, was used to compare length distributions statistically. As fruit ripen, L_N and L_W values from CDTA pectins significantly decreased from 103 nm for green fruit to 75 nm for the red ones. However, L_N and L_W values in Na_2CO_3 fraction were similar at both developmental stages despite the presence at low frequency of longer pectin chains in the contour length distribution of unripe fruit samples.

Branched pectic chains were observed in both pectin fractions from either unripe or ripe fruit; however, its frequency decreased significantly during ripening (Table 2). L_N

and L_W values of branches were not significantly affected by fruit development, being also similar in pectins from CDTA and sodium carbonate fractions.

4. Discussion

4.1. The amount of soluble pectins increases during fruit development

The amount of cell walls per fruit decreased significantly during strawberry development, as previously observed in other studies (Redgwell et al., 1997b; Koh and Melton, 2002; Rosli et al., 2004). Similarly, the yield of all cell wall fractions diminished in ripe fruit when compared with unripe fruit, being the largest decrease observed in the pectin-enriched fractions, i.e. CDTA and sodium carbonate. Interestingly, KOH 4 M fraction, which is enriched in hemicellulosic material, showed the smaller decrease in fraction yield as the fruit ripen. Contrary to the cell wall, the yield of PAW solubilised polymers was similar in both developmental stages. However, taking into account that the CWM amount was much lower in red fruit, this similar PAW yield in a per fruit base indicates a higher solubilisation of the CWM in this developmental stage.

Previous studies found that the amount of soluble pectins, those extracted with PAW or water, increased during strawberry fruit development (Woodward, 1972; Redgwell et al., 1997b; Koh and Melton, 2002). Redgwell et al. (1997b) observed that unripe strawberries contained 35-40 % less PAW soluble pectins than ripe fruit. In addition, the suppression of a polygalacturonase gene, *FaPG1*, reduced the amount of PAW soluble pectins in red fruit while increasing the amount of bound pectins (Posé et al., 2013). PAW fraction represents polymers solubilised by in vivo processes (Redgwell et al., 1992). Our results indicate a solubilisation of pectins during fruit

development. The increase in the polyuronide content in PAW soluble fraction, calculated as the difference in pectin content between unripe and ripe fruit, was 0.37 g kg^{-1} fruit, a similar value to that reported by Redgwell et al. (1997b) for cv. 'Pajaro', 0.62 g kg^{-1} fruit. The amount of pectins soluble in water also increased in ripe fruit. The higher amounts of pectins in PAW and water was paralleled to a decrease in ionically and covalently-bound pectins, suggesting that pectins tightly bound to the cell wall are the main sources of naturally solubilized pectins.

4.2 Several factors contribute to the solubilisation of pectins

Several hypotheses have been formulated to explain the process of pectin solubilisation during fruit ripening, i.e., the loss of arabinan and galactan side chains from RGI, the depolymerisation of chelated or covalently bound pectins, a progressive demethylesterification of HG, or the synthesis of new pectins more soluble (Paniagua et al., 2014).

In this study, the ATR-FTIR profiles of Na_2CO_3 fraction suggest that the amount of neutral sugars decreased as the fruit ripen. The analysis of neutral sugar composition by gas chromatography confirmed that Ara and Gal were the two major components in Na_2CO_3, as well as CDTA fractions, and that Ara decreased notably in ripe fruit. The amount of arabinose was particularly high in the Na_2CO_3 fraction at the unripe stage, suggesting the presence of highly branched arabinans. Koh and Melton (2002) also described a decrease in the Ara content in both pectin fractions during strawberry ripening. The expression of α-L-Arabinofuranosidase and β-Galactosidase genes has been related to the loss of neutral sugars during strawberry ripening (Rosli et al., 2009; Trainotti et al., 2001) and, recently, it has been found that the down-regulation of one of

these β-galactosidase genes increased cell wall galactose content in ripe fruit and reduced strawberry softening (Paniagua et al., 2016).

In regard to pectin depolymerisation, the chromatographic profiles of pectin fractions indicated a reduction in the average molecular weight of polyuronides present in soluble fractions, PAW and water, and in both bound fraction as the fruit ripen. Although the changes in the profiles of the sodium carbonate fractions were smaller and only affected the first peak. Previous size exclusion chromatography analyses of strawberry pectins during ripening yielded contradictory results. Redgwell et al. (1997b) observed a slight depolymerisation of PAW polymers during ripening of strawberry fruit, cv. 'Pajaro', but no change in the CDTA fraction. Figueroa et al. (2010) did not observe any modification in the chromatographic profiles of water soluble polymers from green and ripe fruit, cv. 'Chandler', but they found a depolymerisation of covalently bound pectins extracted with HCl. A similar result was found by Rosli et al. (2004) in 'Toyonaka' fruit, although no depolymerisation of HCl pectins was observed during the ripening of either 'Camarosa' or 'Pajaro' fruit. Despite these contradictory results, a strong support for the role of pectin depolymerisation in the cell wall disassembly process during strawberry fruit ripening has been obtained through the transgenic manipulation of pectinase genes. The silencing of ripening-specific polygalaturonase or pectate lyase genes reduced fruit softening and in the case of bound pectins, this was associated with a higher molecular mass of some population of polymers resolved by size exclusion chromatography and, in general, with longer chains observed by AFM (Santiago-Doménech et al., 2008; Posé et al., 2015).

Pectins are secreted into the wall as highly methylesterified and later processed by pectin methyl esterases (PME), which catalyze their demethylesterification releasing acidic pectins. PME is important in cell wall loosening since polygalacturonase activity

needs blocks of at least four de-esterified galacturonic acid residues (Chen and Mort, 1996). According to Draye and Van Cutsem (2008), the level of methylesterification in strawberry fruit, as well as PME, decreased from the green to the ripe stage. Our results also indicate a decrease in the methylesterification of CDTA pectins during ripening, but the degree of esterification increased in soluble pectins, PAW and water fractions, as the fruit ripen. This result could be explained by the solubilization of ionically bound pectins into more soluble polyuronides during fruit ripening.

4.3. Nanostructural changes in bound pectins during the ripening process

AFM has been used to explore the modifications of pectin structure during ripening of several fruit (Yang et al., 2009; Zareie et al., 2003). Pectins are usually visualized in AFM images as linear chains and micellar aggregates. It has been proposed that strands, backbone and branches, are mainly formed by polygalacturonic acid while micellar aggregates are complex structures formed by HG and RGI (Round et al., 2001; Round et al., 2010; Paniagua et al., 2017). CDTA linear chains were longer than those observed in the carbonate fraction samples at both developmental stages, as previously observed in ripe strawberry (Posé et al., 2012) and peach (Yang et al., 2009) or unripe tomato (Kirby et al., 2008). The analysis of AFM images from CDTA samples revealed that linear chains from unripe fruit were significantly longer than those from ripe fruit. The percentage of CDTA branched chains also decreased significantly in ripe fruit. By contrast, the median values of the pectic chains present in carbonate fraction samples were similar at both developmental stages, suggesting that these pectins are not depolymerised during fruit development. Although L_N and L_W values were similar in unripe and ripe carbonate pectins, contour length distributions were slightly different; the unripe samples showed a small proportion of long pectic chains, higher than 300 nm

length, that were not present in samples from red fruit. However, the most noticeable change detected by AFM in carbonate fraction was the decrease in the percentage of branched chains, from 19 to 3 % in unripe and ripe samples, respectively, and the reduction in the number of micellar aggregates. Altogether, AFM results show that the structural complexity of ionically and covalently bound pectins is substantially reduced as the fruit ripen. The degradation of the pectin matrix continues after harvest during fruit storage; Chen et al. (2011) observed that pectin chain widths and lengths decreased during strawberry storage at 4 ºC for 15 d, contributing to the loss of fruit firmness. Pectinase enzymes such as polygalacturonase and pectate lyase should be involved in the disassembly of bound pectins, since the structural features of pectins in transgenic ripe fruit with low expression levels of these genes, reported by Posé et al. (2015), resemble the characteristics here described for unripe fruit.

4.4. Conclusions

The increase in soluble pectins at the expense of ionically (CDTA fraction) and covalently (Na_2CO_3 fraction) bound polyuronides is the main cell wall change taking place during the transition from green-unripe to red-ripe strawberry fruit. The chromatographic analysis of pectin fractions indicates that CDTA pectins were depolymerised in ripe fruit, but not Na_2CO_3 polyuronides. Additionally, the amount of Ara was notably reduced in both fractions at the ripe stage. The nanostructure of bound pectins has been analysed by AFM. The results obtained suggest a reduction of the structural complexity of pectins during fruit development. Thus, pectic chains displayed a lower number of branches and the number of pectin aggregates was reduced in the samples of red fruit. This set of chemical, biochemical and nanostructural changes of the pectin matrix during ripening could contribute to the pectin solubilisation process

and to the modification of the cell wall physical properties, probably reducing its mechanical strength and, finally, leading to a reduction in fruit firmness.

Acknowledgements

This work was supported by the Ministerio de Economía y Competitividad of Spain and FEDER EU Funds (grant reference AGL2014-55784-C2-1-R) and by a Ramón y Cajal project RYC-2011-08839 awarded to AJM. The use of AFM was supported by the Biotechnology and Biological Science Research Council (BBSRC) through its core strategic grant to IFR. Authors thank Dr. K.W. Waldron (Institute of Food Research, UK) for his help in the neutral sugar analysis.

References

Adams, E.L., Kroon, P.A., Williamson, G., Morris, V.J., 2003. Characterisation of heterogeneous arabinoxylans by direct imaging of individual molecules by atomic force microscopy. Carbohyd. Res., 338, 771-780.

Blakeney, A.B, Harris, P.J., Henry, R.J., Stone, B.A., 1983. A simple and rapid preparation of alditol acetates for monosaccharide analysis. Carbohyd. Res., 113, 291-299.

Brummell, D.A., 2006. Cell wall disassembly in ripening fruit. Funct. Plant Biol. 33, 103-119.

Chen, E.M.W., Mort, J. A., 1996. Nature of sites hydrolyzable by endopolygalacturonase in partially-esterified homogalacturonans. Carbohyd. Polym., 29, 129-136.

Chen, F., Liu, H., Yang, H., Lai, S., Cheng, X., Xin, Y., Yang, B., Hou, H., Yao, Y., Zhang, S., Bu, G., Deng, Y., 2011. Quality attributes and cell wall properties of strawberries (*Fragaria annanassa* Duch.) under calcium chloride treatment. Food Chem. 126, 450-459.

Draye, M., Van Cutsem, P., 2008. Pectin methylesterases induce an abrupt increase of acidic pectin during strawberry fruit ripening. J. Plant Physiol. 165, 1152-1160.

Figueroa, C.R., Rosli, H.G., Civello, P.M., Martínez, G.A., Herrera, R., Moya-León, M.A., 2010. Changes in cell wall polysaccharides and cell wall degrading enzymes during ripening of *Fragaria chiloensis* and *Fragaria* × *ananassa* fruits. Sci. Hort. 124, 454-462.

Filisetti-Cozzi, T.M.C.C., Carpita, N.C., 1991. Measurement of uronic acids without interference from neutral sugars. Anal. Biochem. 197, 157-162.

Gapper, N.E., McQuinn, R.P., Giovannoni, J.J., 2013. Molecular and genetic regulation of fruit ripening. Plant Mol. Biol. 82, 575-591.

Goulao, L.F., Oliveira, C.M., 2008. Cell wall modification during fruit ripening: when a fruit is not the fruit. Trends Food Sci. Tech., 19, 4-25.

Gross, K.C., Sams, C.E., 1984. Changes in cell wall neutral sugar composition during fruit ripening: a species survey. Phytochemistry 23, 2457-2461.

Huber, D.J., 1984. Strawberry (*Fragaria x ananassa*) fruit softening, the potential roles of polyuronides and hemicelluloses. J. Food Sci. 49, 1310-1315.

Jiménez-Bermúdez, S., Redondo-Nevado, J., Muñoz-Blanco, J., Caballero, J.L., López-Aranda, J.M., Valpuesta, V., Pliego-Alfaro, F., Quesada, M.A., Mercado, J.A., 2002. Manipulation of strawberry fruit softening by antisense expression of a pectate lyase gene. Plant Physiol. 128, 751-759.

Kacuráková, M., Capek, P., Sasinková, V., Wellner, N., & Ebringerová, A., 2000. FT-IR study of plant cell wall model compounds: Pectic polysaccharides and hemicelluloses. Carbohyd. Polym. 43, 195-203.

Kho, T.H., Melton, L.D., 2002. Ripening-related changes in cell wall polysaccharides of strawberry cortical and pith tissues. Postharvest Biol. Technol. 26, 23-33.

Kirby, A.R., Gunning, A.P., Morris, V.J., 1996. Imaging polysaccharides by atomic force microscopy. Biopolym., 38, 355-366.

Kirby, A.R., MacDougall, A.J., Morris, V.J., 2008. Atomic force microscopy of tomato and sugar beet pectin molecules. Carbohydr. Polym. 71, 640-647.

Lee, C.H., Min, J.H., Kim, T.I., Kim, J.G., Matsumoto, K., Kim, D.Y., Hwang, Y.S., 2011. Comparison of wall polymers among three genetically closely related strawberry cultivars with different fruit firmness. Hort. Environ. Biotechnol. 52, 581-589.

Mercado, J.A., Pliego-Alfaro, F., Quesada, M.A., 2011. Fruit shelf life and potential for its genetic improvement, in: Jenks, M.A., Bebeli, P.J. (Eds.), Breeding for Fruit Quality. Oxford, John Wiley & Sons, Inc., pp. 81-104.

Paniagua, C., Posé, S., Morris, V.J., Kirby, A.R., Quesada, M.A., Mercado, J.A., 2014. Fruit softening and pectin disassembly: an overview of nanostructural pectin modifications assessed by atomic force microscopy. Ann. Bot. 114, 1375-1383.

Paniagua, C., Blanco-Portales, R., Barceló-Muñoz, M., García-Gago, J.A., Waldron, K. W., Quesada, M.A., Muñoz-Blanco, J., Mercado, J.A., 2016. Antisense down-regulation of the strawberry β-galactosidase gene FaβGal4 increases cell wall galactose levels and reduces fruit softening. J. Exp. Bot. 67, 619-631.

Paniagua, C., Kirby, A.R., Gunning, A.P., Morris, V.J., Matas, A.J., Quesada, M.A., Mercado, J.A. 2017. Unravelling the nanostructure of strawberry fruit pectins by

endo-polygalacturonase digestion and atomic force microscopy. Food Chem. 224, 270-279.

Posé, S., García-Gago, J.A., Santiago-Doménech, N., Pliego-Alfaro, F., Quesada, M.A., Mercado, J.A., 2011. Strawberry fruit softening: role of cell wall disassembly and its manipulation in transgenic plants. Genes, Genomes and Genomics 5, 40-48.

Posé, S., Kirby, A. R., Mercado, J. A., Morris, V. J., Quesada, M. A., 2012. Structural characterization of cell wall pectin fractions in ripe strawberry fruits using AFM. Carbohyd Polym, 88, 882-890.

Posé, S., Paniagua, C., Cifuentes, M., Blanco-Portales, R., Quesada, M. A., Mercado, J. A., 2013. Insights into the effects of polygalacturonase *FaPG1* gene silencing on pectin matrix disassembly, enhanced tissue integrity, and firmness in ripe strawberry fruits. J. Exp. Bot., 64, 3803-3815.

Posé S, Kirby AR, Paniagua C, Waldron KW, Morris VJ, Quesada MA, Mercado JA. 2015. The nanostructural characterization of strawberry pectins in pectate lyase or polygalacturonase silenced fruits elucidates their role in softening. Carbohydr. Polym. 132, 134-145.

Quesada, M.A., Blanco-Portales, R., Posé, S., García-Gago, J.A., Jiménez-Bermúdez, S., Muñoz-Serrano, A., Caballero, J.L., Pliego-Alfaro, F., Mercado, J.A., Muñoz-Blanco, J., 2009. Antisense down-regulation of the *FaPG1* gene reveals an unexpected central role for polygalacturonase in strawberry fruit softening. Plant Physiol. 150, 1022-1032.

Redgwell, R.J., Melton, L.D., Brasch, D.J., 1992. Cell-wall dissolution in ripening kiwifruit (*Actinidia deliciosa*). Solubilisation of the pectic polymers. Plant Physiol. 98, 71-81.

Redgwell, R.J., Fischer, M., Kendall, E., MacRae, E.A., Perry, J., Harker, R., 1997a. Galactose loss and fruit ripening: high-molecular-weight arabinogalactans in the pectic polysaccharides of fruit cell walls. Planta 203, 174-181.

Redgwell, R.J., MacRae, E.A., Hallett, I., Fischer, M., Perry, J., Harker, R., 1997b. *In vivo* and *in vitro* swelling of cell walls during fruit ripening. Planta 203, 162-173.

Rimington, C., 1931. The carbohydrate complex of the serum proteins: Improved method for isolation and re-determination of structure. Isolation of glucosaminodimannose from proteins of ox blood. Biochem. J. 25, 1062-1071.

Rose, J.K.C., Hadfield, K.A., Labavitch, J.M., Bennett, A.B., 1998. Temporal sequence of cell wall disassembly in rapidly ripening melon fruit. Plant Physiol. 117, 345-361.

Rosli, H.G., Civello, P.M., Martinez, G.A., 2004. Changes in cell wall composition of three *Fragaria x ananassa* cultivars with different softening rate during ripening. Plant Physiol. Biochem. 42, 823-831.

Rosli, H.G., Civello, P.M., Martinez, G.A., 2009. α-L-Arabinofuranosidase from strawberry fruit: Cloning of three cDNAs, characterization of their expression and analysis of enzymatic activity in cultivars with contrasting firmness. Plant Physiol. Biochem. 47, 272-281.

Round, A. N., Rigby, N. M., MacDougall, A. J., Ring, S. G., Morris, J. V., 2001. Investigating the nature of branching in pectin by atomic force microscopy and carbohydrate analysis. Carbohyd. Res., 331, 337-342.

Round, A. N., Rigby, N. M., MacDougall, A. J., Morris, V. J., 2010. A new view of pectin structure revealed by acid hydrolysis and atomic force microscopy. Carbohyd. Res., 345,487-497.

Santiago-Doménech, N., Jiménez-Bermúdez, S., Matas, A.J., Rose, J.K.C., Muñoz-Blanco, J., Mercado, J.A., Quesada, M.A., 2008. Antisense inhibition of a pectate

lyase gene supports a role for pectin depolymerization in strawberry fruit softening. J. Exp. Bot. 59, 2769-2779.

Smith, D.L., Abbott, J.A., Gross, K.C., 2002. Down-regulation of tomato β-galactosidase 4 results in decreased fruit softening. Plant Physiol. 129, 1755-1762.

Trainotti, L., Spinello, R., Piovan, A., Spolaore, S., Casadoro, G., 2001. β-galactosidases with a lectin-like domain are expressed in strawberry. J. Exp. Bot. 52, 1635-1645.

Vicente, A.R., Ortugno, C., Powell, A.L.T., Greve, L.C., Labavitch, J.M., 2007. Temporal sequence of cell wall disassembly events in developing fruits. 1. Analysis of raspberry (*Rubus idaeus*). J. Agric. Food Chem. 55, 4119-4124.

Woodward, J.R., 1972. Physical and chemical changes in developing strawberry fruits. J. Sci. Food Agric., 23, 465-473.

Yang, H., Chen, F., An, H., Lai, S., 2009. Comparative studies on nanostructures of three kinds of pectins in two peach cultivars using atomic force microscopy. Postharvest Biol. Technol. 51, 391-398.

Zareie, M.H., Gokmen V, Javadipour I. 2003. Investigating network, branching, gelation and enzymatic degradation in pectin by atomic force microscopy. J. Food Sci. Technol. 40, 169-172.

Table 1. Descriptors of contour length distribution of CDTA and sodium carbonate pectins extracted from unripe and ripe strawberry fruit obtained from AFM images. ME correspond to the median of the original data. For each pectin fraction, ME values with different letters indicate significant differences by Kruskal-Wallis non-parametric median test at P=0.05.

	Unripe	Ripe
CDTA		
L_N (nm)	116.3	90.9
L_W (nm)	148.5	113.6
PDI	1.3	1.2
ME (nm)	102.9a	75.5b
Sodium carbonate		
L_N (nm)	79.8	78.7
L_W (nm)	104.1	102.0
PDI	1.3	1.3
ME (nm)	69.8a	69.2a

Table 2: Percentages of linear chains with branches and descriptors of contour length distribution of the branches from CDTA and sodium carbonate soluble pectins extracted from unripe and ripe strawberry fruit. Data obtained from AFM images. Branching percentages differences were statistically analyzed by Chi-squared test at P=0.05

	Unripe	Ripe
CDTA		
Branching (%)	12.9a	3.2b
L_N (nm)	35.7	41.1
L_W (nm)	51.1	47.3
PDI	1.4	1.2
Sodium carbonate		
Branching (%)	19.7a	3.4b
L_N (nm)	35.9	28.6
L_W (nm)	48.0	39.8
PDI	1.3	1.4

Figure legends

Figure 1: (A) A representative image of the two developmental stages analyzed, unripe-green and ripe-red fruit. Bar corresponds to 1 cm. (B) Amount of the different fractions obtained after sequential extraction of CWM from unripe and ripe fruit. Data correspond to mean ± SD. Within each fraction, columns with different letters are significantly different by the Tukey-HSD test at P=0.05.

Figure 2: Amount of uronic acids (A) and neutral sugars (B) in the cell wall fractions extracted from unripe and ripe fruit. Data correspond to mean ± SD. Within each fraction, columns with different letters are significantly different by the Tukey-HSD test at P=0.05.

Figure 3: ATR-FTIR spectra of the different pectin fractions extracted from unripe and ripe fruit in the region 2000-800 cm^{-1}.

Figure 4: Chromatographic elution profiles of the different pectin fractions extracted from unripe and ripe fruit. Profiles were obtained by size exclusion chromatography on Sepharose CL-6B (PAW and water fractions) or CL-2B (CDTA and Na_2CO_3 fractions). Fractions were assayed for uronic acid and expressed as relative optical density (OD) at 515 nm. Arrows indicate the elution volume for the blue dextran standard (2000 kDa).

Figure 5: Neutral sugar composition in mol % of CDTA and sodium carbonate pectin fractions isolated from unripe and ripe strawberry fruit. Bars represent mean±SD of three independent measurements.

Figure 6: Representative topographical AFM images of CDTA and sodium carbonate soluble pectins extracted from cell walls of green-unripe and red-ripe fruit. The scale bars correspond to 100 nm. A-F: Detailed images of linear unbranched chains (A, B), branched chains (C, D) and micellar aggregates (E, F).

Figure 7: Contour length distributions of CDTA and sodium carbonate soluble samples isolated from fruit cell walls of unripe and ripe fruit. Bars represent relative frequencies of the observed data.

Contribution

CP and NS-D were responsible for conducting the cell wall analyses

ARK, APG and VM contributed to the experiments of AFM

MAQ, AJM and JAM designed the experiments and wrote the manuscript

Figure 1

Click here to download high resolution image

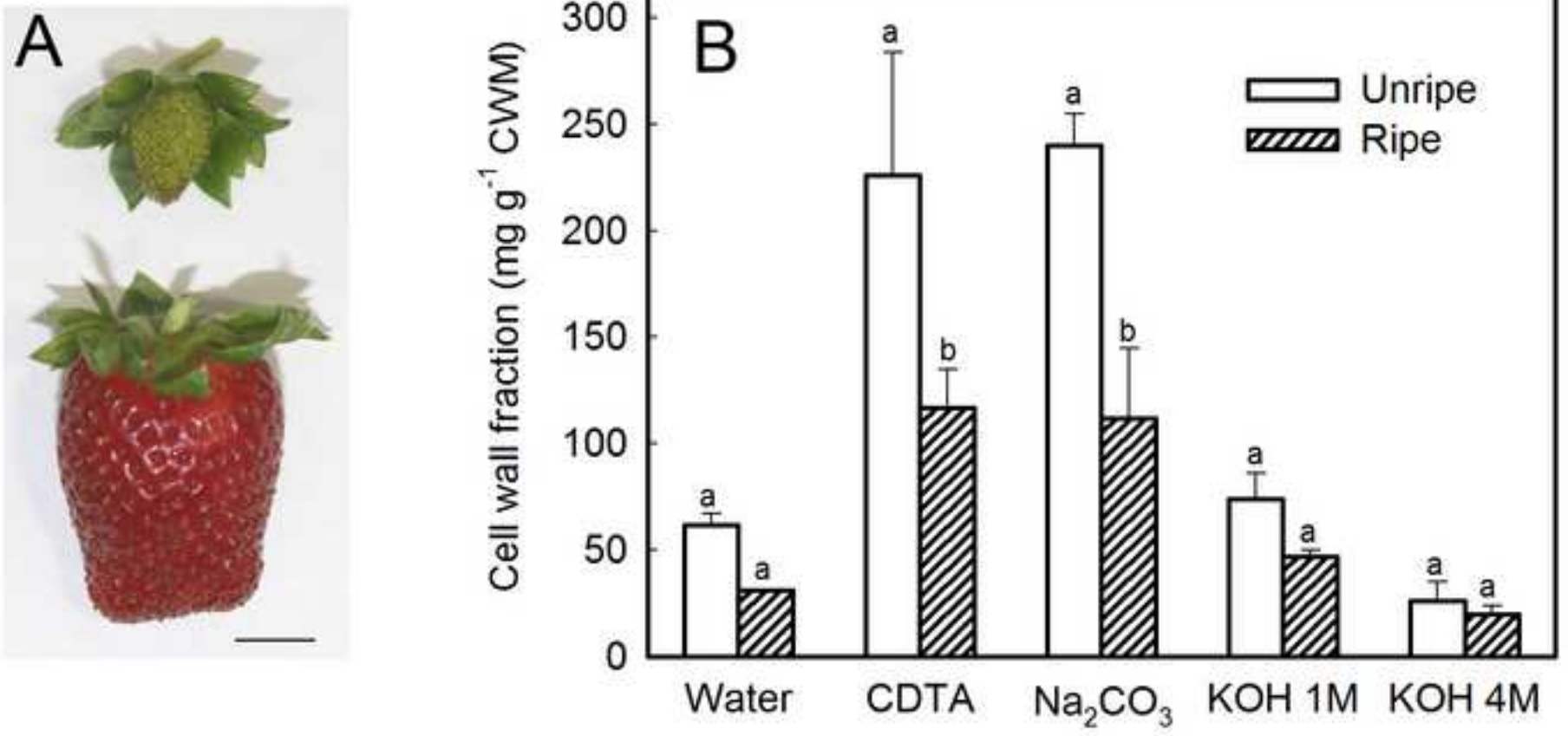

Figure 2

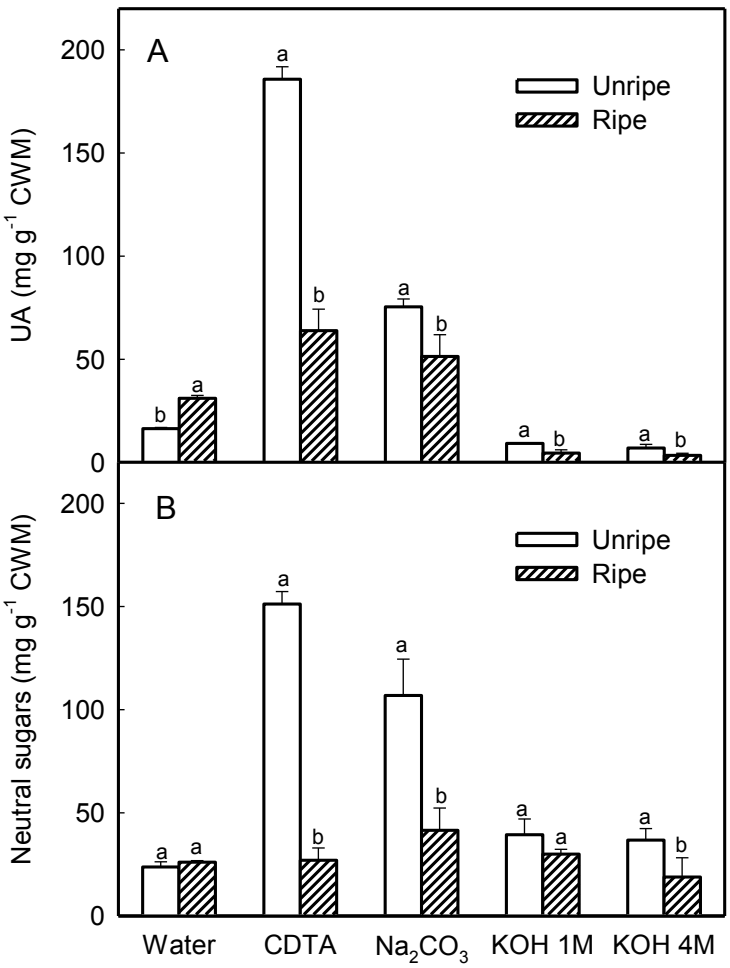
A
B
Unripe
Ripe
UA (mg g-1 CWM)
Neutral sugars (mg g-1 CWM)
0
50
100
150
200
a
b
Water
CDTA
Na2CO3
KOH 1M
KOH 4M

Figure 3

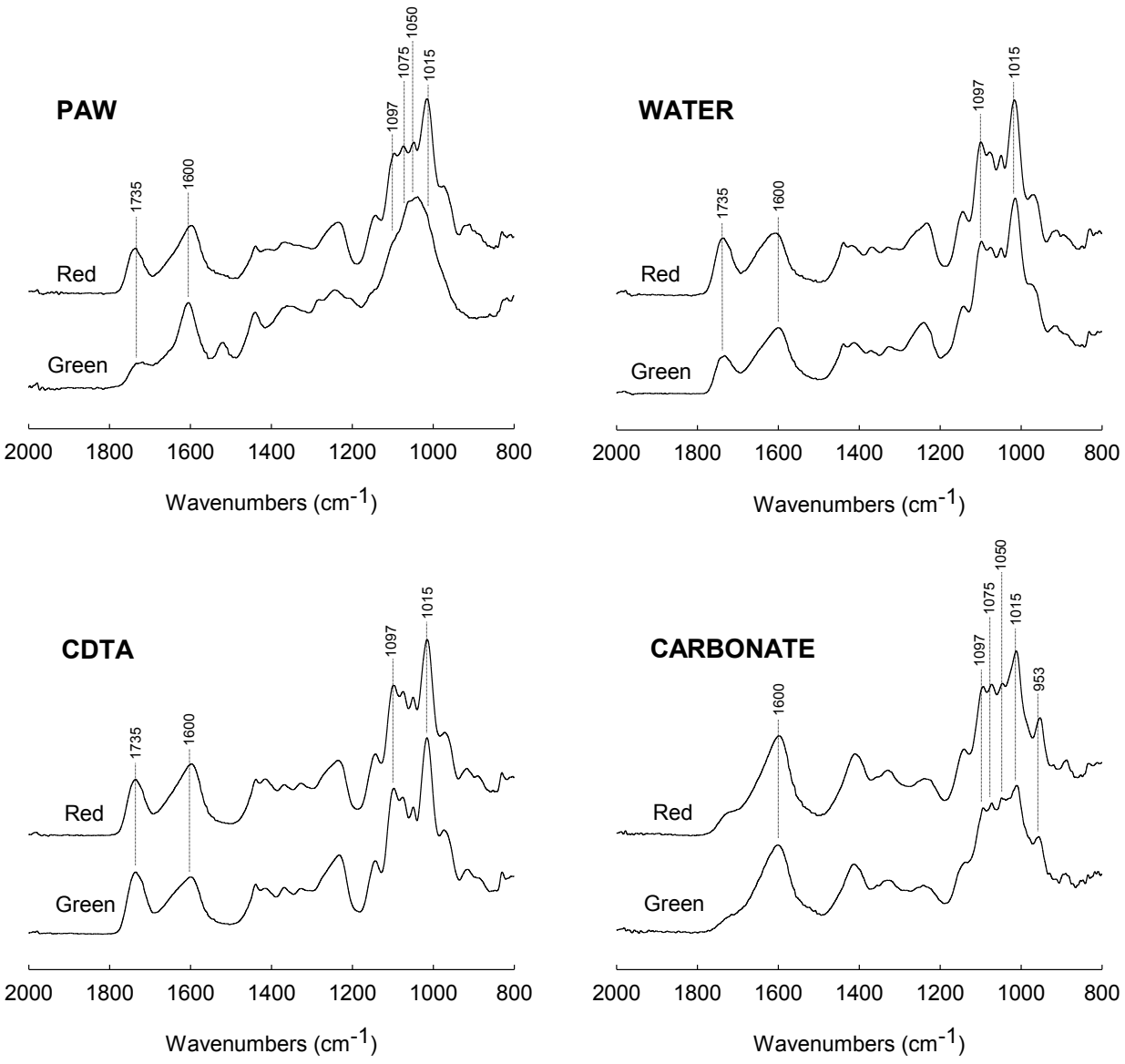
PAW
1735
1600
1097
1075
1050
1015
Red
Green
2000 1800 1600 1400 1200 1000 800
Wavenumbers (cm-1)
WATER
1735
1600
1097
1015
Red
Green
2000 1800 1600 1400 1200 1000 800
Wavenumbers (cm-1)
CDTA
1735
1600
1097
1015
Red
Green
2000 1800 1600 1400 1200 1000 800
Wavenumbers (cm-1)
CARBONATE
1600
1097
1075
1050
1015
953
Red
Green
2000 1800 1600 1400 1200 1000 800
Wavenumbers (cm-1)

Figure 4

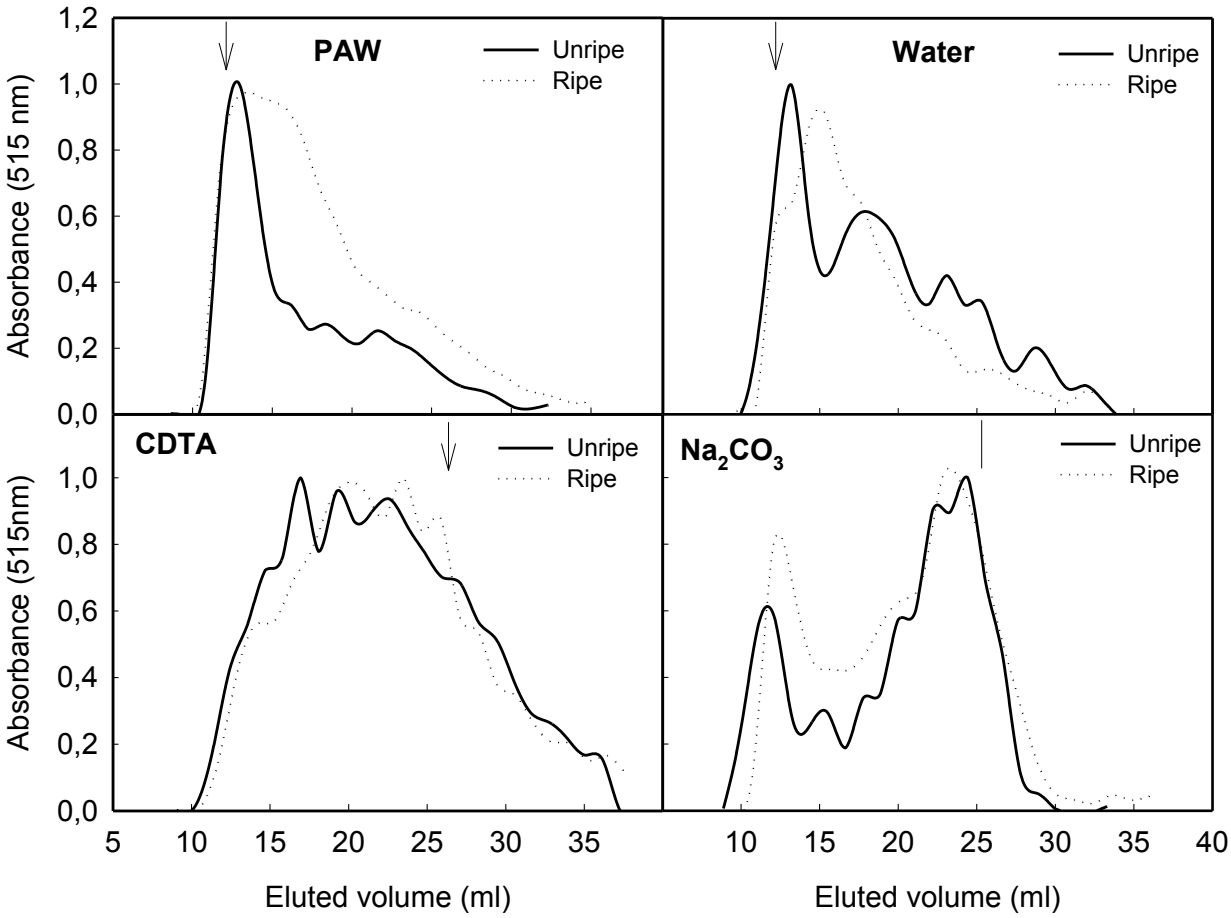
PAW
Water
CDTA
Na_2CO_3
Unripe
Ripe
Absorbance (515 nm)
Absorbance (515nm)
Eluted volume (ml)
Eluted volume (ml)
1,2
1,0
0,8
0,6
0,4
0,2
0,0
5
10
15
20
25
30
35
40

Figure 5

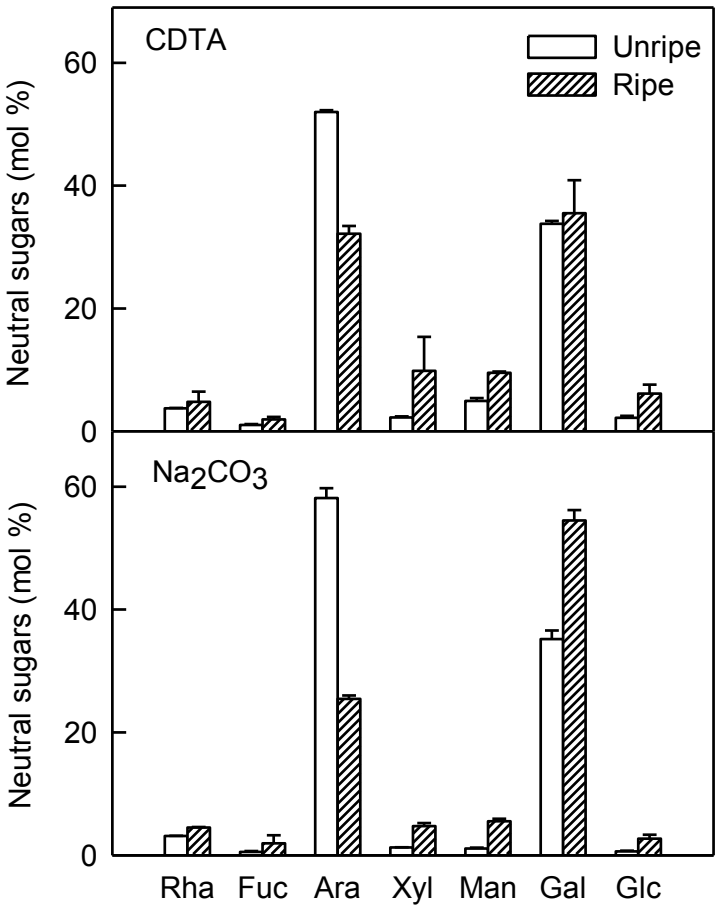
CDTA
Unripe
Ripe
Neutral sugars (mol %)
60
40
20
0
Na2CO3
Neutral sugars (mol %)
60
40
20
0
Rha
Fuc
Ara
Xyl
Man
Gal
Glc

Figure 6

Click here to download high resolution image

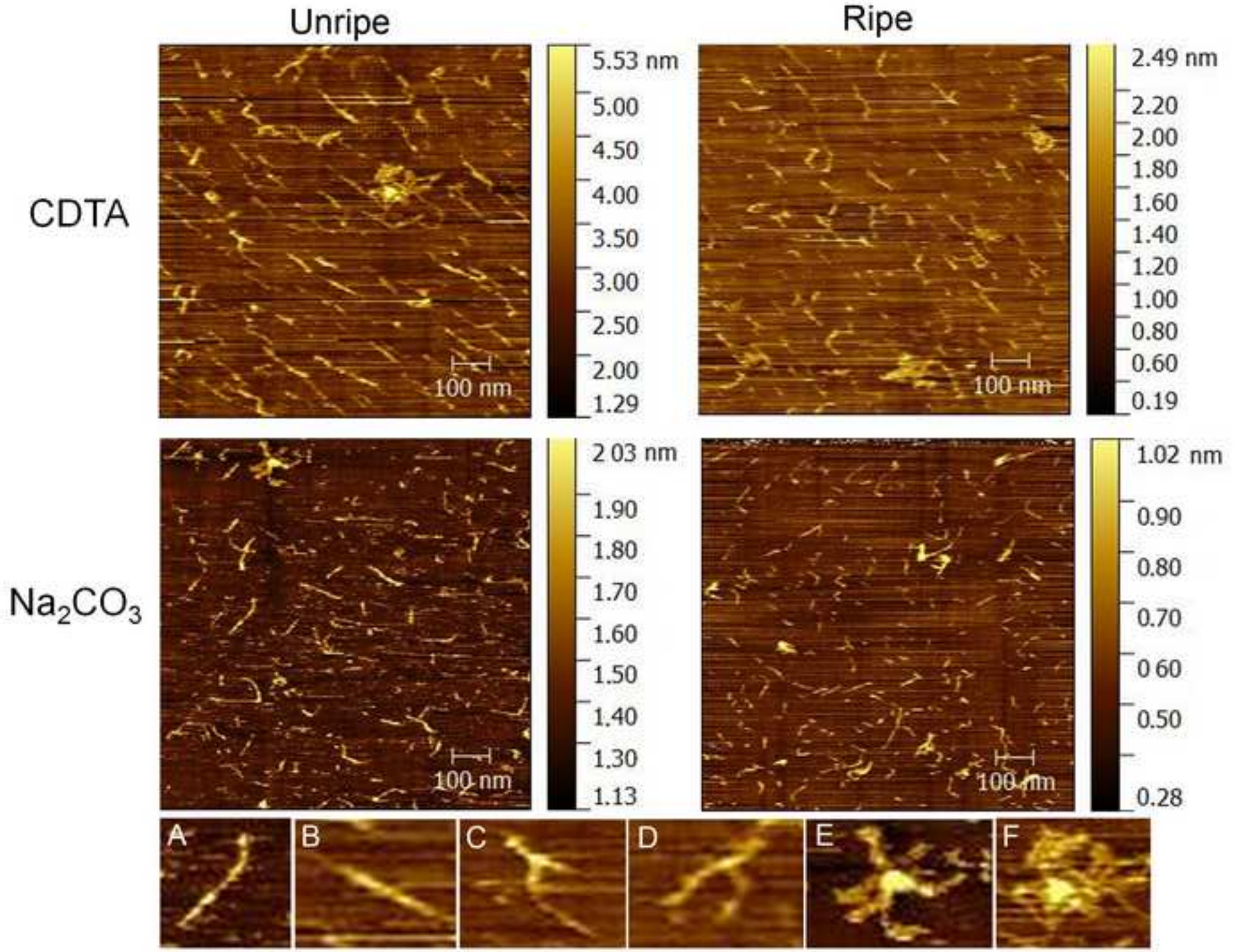

Figure 7

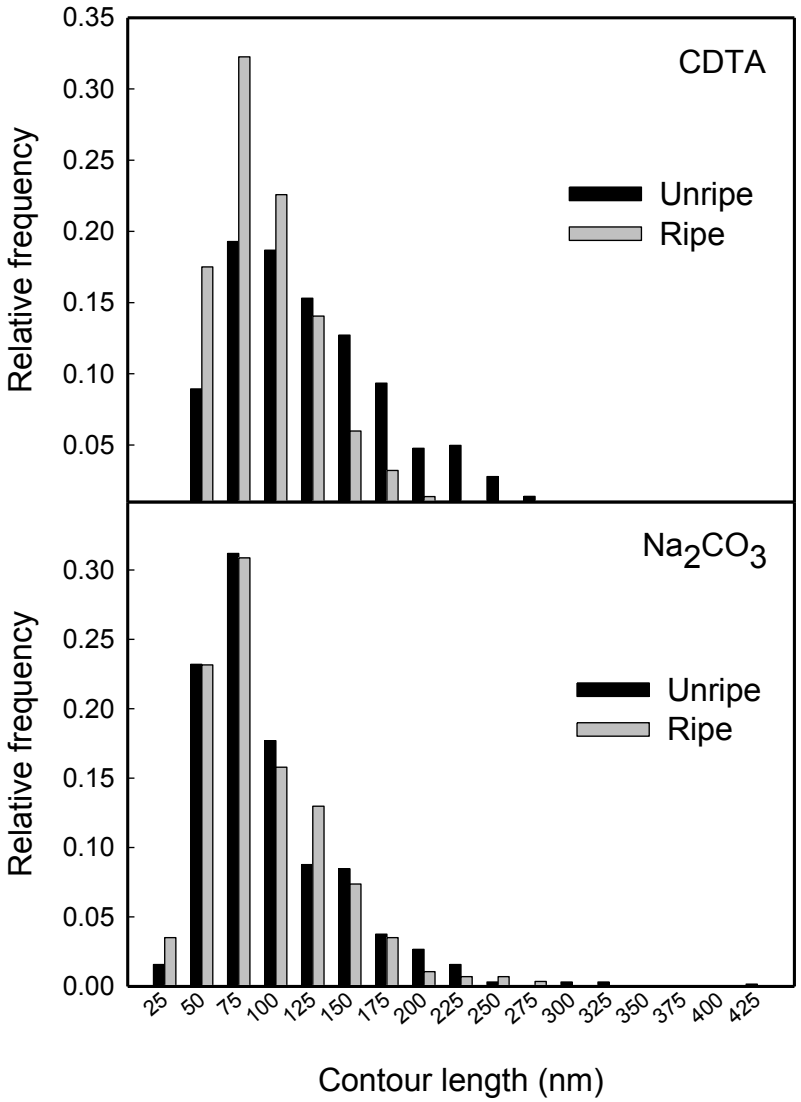
CDTA
Unripe
Ripe
Relative frequency
0.35
0.30
0.25
0.20
0.15
0.10
0.05
Na2CO3
Unripe
Ripe
Relative frequency
0.30
0.25
0.20
0.15
0.10
0.05
0.00
25
50
75
100
125
150
175
200
225
250
275
300
325
350
375
400
425
Contour length (nm)